

AD-A217 769

# Geometric Scale of Interaction Between Moving Shock and Stationary Thermal Layer

Prepared by

H. MIRELS  
Aerophysics Laboratory

1 November 1989

Laboratory Operations  
THE AEROSPACE CORPORATION  
El Segundo, CA 90245

SDTIC  
ELECTE  
FEB 07 1990  
S E D

Prepared for

DEFENSE NUCLEAR AGENCY  
Alexandria, VA 22310-1000

Statement A  
for public release;  
Distribution unlimited.



THE AEROSPACE CORPORATION

## LABORATORY OPERATIONS

The Aerospace Corporation functions as an "architect-engineer" for national security projects, specializing in advanced military space systems. Providing research support, the corporation's Laboratory Operations conducts experimental and theoretical investigations that focus on the application of scientific and technical advances to such systems. Vital to the success of these investigations is the technical staff's wide-ranging expertise and its ability to stay current with new developments. This expertise is enhanced by a research program aimed at dealing with the many problems associated with rapidly evolving space systems. Contributing their capabilities to the research effort are these individual laboratories:

Aerophysics Laboratory: Launch vehicle and reentry fluid mechanics, heat transfer and flight dynamics; chemical and electric propulsion, propellant chemistry, chemical dynamics, environmental chemistry, trace detection; spacecraft structural mechanics, contamination, thermal and structural control; high temperature thermomechanics, gas kinetics and radiation; cw and pulsed chemical and excimer laser development including chemical kinetics, spectroscopy, optical resonators, beam control, atmospheric propagation, laser effects and countermeasures.

Chemistry and Physics Laboratory: Atmospheric chemical reactions, atmospheric optics, light scattering, state-specific chemical reactions and radiative signatures of missile plumes, sensor out-of-field-of-view rejection, applied laser spectroscopy, laser chemistry, laser optoelectronics, solar cell physics, battery electrochemistry, space vacuum and radiation effects on materials, lubrication and surface phenomena, thermionic emission, photo-sensitive materials and detectors, atomic frequency standards, and environmental chemistry.

Computer Science Laboratory: Program verification, program translation, performance-sensitive system design, distributed architectures for spaceborne computers, fault-tolerant computer systems, artificial intelligence, microelectronics applications, communication protocols, and computer security.

Electronics Research Laboratory: Microelectronics, solid-state device physics, compound semiconductors, radiation hardening; electro-optics, quantum electronics, solid-state lasers, optical propagation and communications; microwave semiconductor devices, microwave/millimeter wave measurements, diagnostics and radiometry, microwave/millimeter wave thermionic devices; atomic time and frequency standards; antennas, rf systems, electromagnetic propagation phenomena, space communication systems.

Materials Sciences Laboratory: Development of new materials: metals, alloys, ceramics, polymers and their composites, and new forms of carbon; non-destructive evaluation, component failure analysis and reliability; fracture mechanics and stress corrosion; analysis and evaluation of materials at cryogenic and elevated temperatures as well as in space and enemy-induced environments.

Space Sciences Laboratory: Magnetospheric, auroral and cosmic ray physics, wave-particle interactions, magnetospheric plasma waves; atmospheric and ionospheric physics, density and composition of the upper atmosphere, remote sensing using atmospheric radiation; solar physics, infrared astronomy, infrared signature analysis; effects of solar activity, magnetic storms and nuclear explosions on the earth's atmosphere, ionosphere and magnetosphere; effects of electromagnetic and particulate radiations on space systems; space instrumentation.

Aerospace Report No.  
ATR-89(4785)-1

GEOMETRIC SCALE OF INTERACTION BETWEEN  
MOVING SHOCK AND STATIONARY THERMAL LAYER

Prepared by

H. Mirels  
Aerophysics Laboratory

1 November 1989

Laboratory Operations  
THE AEROSPACE CORPORATION  
El Segundo, CA 90245

Statement A  
Approved for public release;  
Distribution unlimited. \_\_\_\_\_

Prepared for

DEFENSE NUCLEAR AGENCY  
Alexandria, VA 22310-1000

GEOMETRIC SCALE OF INTERACTION BETWEEN  
MOVING SHOCK AND STATIONARY THERMAL LAYER

Prepared

H. Mirels  
H. Mirels

Approved

R. W. Fillers  
R. W. Fillers, Director  
Aerophysics Laboratory

Accession For	
NTIS GRA&I	<input checked="" type="checkbox"/>
DTIC TAB	<input type="checkbox"/>
Unannounced	<input type="checkbox"/>
Justification	
By	
Distribution/	
Availability Codes	
Dist	Avail and/or Spec
A-1	



## ABSTRACT

An analytical model is presented for estimating the streamwise length of the steady-state separation bubble induced by the interaction of a shock moving with constant speed over a thin thermal (high sound speed) layer. In the case of a thermal layer of semi-infinite extent, the steady solution represents the asymptotic limit of an initially unsteady interaction. The streamwise length of the separation bubble is found by equating mass flow into the bubble to the mass flow removed by the wall boundary layer. Numerical results are presented for a variety of shock speeds, thermal layer heights, and thermal layer sound speeds. The present study indicates the importance of viscous effects on precursor development and provides a method for modifying the wall boundary condition in inviscid numerical codes in order to include the effect of the wall boundary layer on the inviscid flow field.

PREFACE

Funding for this effort was processed through SSD Contract No. F04701-88-C-0089 under an Interagency Agreement from the Defense Nuclear Agency.

CONTENTS

ABSTRACT.....	v
PREFACE.....	vii
I. INTRODUCTION.....	1
II. THEORY.....	3
III. TIME TO REACH STEADY STATE.....	21
IV. APPLICATION TO NUMERICAL CODES.....	23
V. CONCLUDING REMARKS.....	25
REFERENCES.....	27
APPENDIX: SYMBOLS.....	29

## FIGURES

1. Initial Conditions in Laboratory Stationary Coordinate System.....	4
2. Flow Conditions in Incident Shock Stationary Coordinate System at Early Times.....	5
3. Flow Conditions in Incident Shock Stationary Coordinate System at Late Times.....	6
4. Wall Boundary Layer in Incident Shock Fixed Coordinate System.....	8
5. Boundary Layer Development with Transition at $\xi_t$ and with Effective Origin of Turbulent Boundary Layer at $\xi_0$ .....	10
6. Streamwise Length of Separation Bubble for Case $\gamma_4 = 7/5$ , $\omega = 0.7$ , and $Re_t = 10^6$ .....	16-18

## TABLES

1. Asymptotic Length of Thermal Precursor for Case $\gamma_4 = 7/5$ , $\omega = 0.7$ , and $Re_t = 10^6$ .....	14-15
2. Characteristic Time to Reach Steady State for Case $\gamma_1 = \gamma_4 = 7/5$ .....	19

## I. INTRODUCTION

The interaction between a moving shock wave and a thin thermal (high sound speed) layer results in a precursor wave system, as first discussed by Hess.<sup>1</sup> Experimental studies of this interaction are reported in Refs. 2-4. Numerical code calculations, which assume inviscid flow, are presented in Refs. 5-7.

In Ref. 8, a simple analytical model was presented that neglected viscous effects and that was in approximate agreement with the inviscid code calculations in Ref. 5. The inviscid model and the inviscid code calculations indicate that the scale of the interaction increases linearly with time. In Ref. 8, it was pointed out that viscous effects are expected to cause the scale to approach an asymptotic limit. In this limit, the flow is steady in shock fixed coordinates. The asymptotic scale is estimated in the present study by consideration of wall boundary layer effects. The time to reach steady state is also estimated. Finally, the application of the present results to inviscid codes is discussed. Symbols are defined in the Appendix.

## II. THEORY

Consider a normal shock wave that moves with uniform velocity  $\bar{u}_s$  over a thin thermal layer of semi-infinite extent. Flow conditions prior to the start of the interaction are indicated in Fig. 1, using a laboratory stationary coordinate system. In this coordinate system, flow velocities are denoted by a superscript bar. The thermal layer is characterized by a speed of sound  $a_4$ , which is higher than the adjacent fluid value  $a_1$ .

For cases other than  $a_4/a_1 - 1$  small and/or  $\bar{u}_s/a_1 - 1$  small, a shock is generated in the thermal layer that moves faster than the incident shock and thereby creates a "precursor" flow field.<sup>1,8</sup> The precursor flow field at small times, when viscous effects are negligible, is illustrated in Fig. 2, using a coordinate system wherein the incident shock is stationary. Velocities in this coordinate system are denoted by the unbarred symbol  $u$ . The total head of the thermal layer fluid in region 4 is less than the static pressure in region 2. Consequently, the high pressure gas from region 2 expands into region 3 and drives a shock in the thermal layer. The leading edge of the driver gas is denoted  $x_i$ , and the thermal layer shock location is denoted  $x_{st}$ . The quantities  $x_{sp}$  and  $x_s$  denote a rear stagnation point and incident shock location, respectively. The thermal layer gas collects in the form of a bubble beneath the incident shock. Inviscid numerical code calculations<sup>5</sup> indicate that the interface velocity  $u_i$  and the thermal layer shock velocity  $u_{st}$  are equal and remain constant with time. As a consequence, the separation distance  $x_{st} - x_i$  remains constant. An analytic model of the precursor flow field was presented in Ref. 8 by analogy with a low pressure shock tube flow wherein the separation distance between shock and contact surface remains constant.

Inviscid solutions for the precursor flow field indicate that the scale of the interaction grows linearly with time. As noted in Ref. 8, viscous effects will cause the scale to approach an asymptotic limit. In this limit, the rate of mass flow into the interaction region equals the rate of mass flow out of the interaction region because of the wall boundary layer. This steady state asymptotic limit is illustrated in Fig. 3, using an incident shock fixed coordinate system. In this coordinate system, the wall moves with velocity  $u_w = u_1 = \bar{u}_s$ . The wall boundary layer may be viewed as aspirating mass from

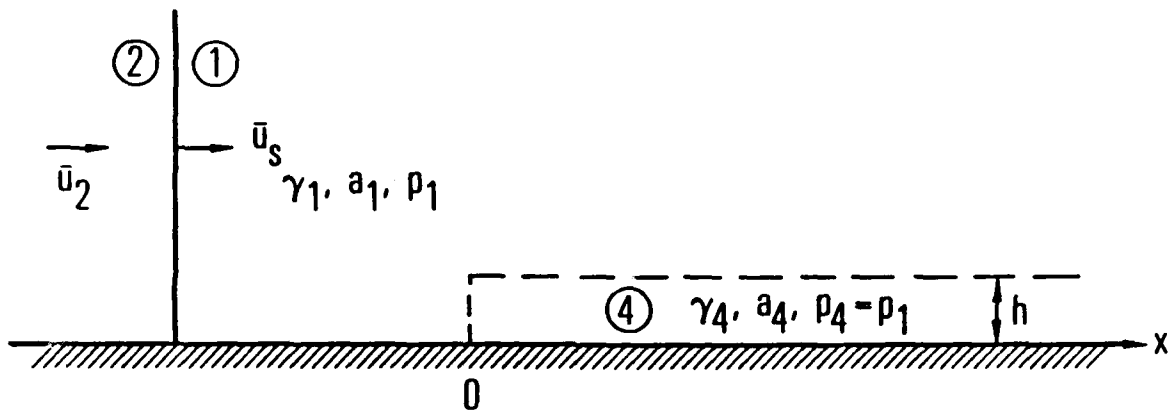


Fig. 1. Initial Conditions in Laboratory Stationary Coordinate System

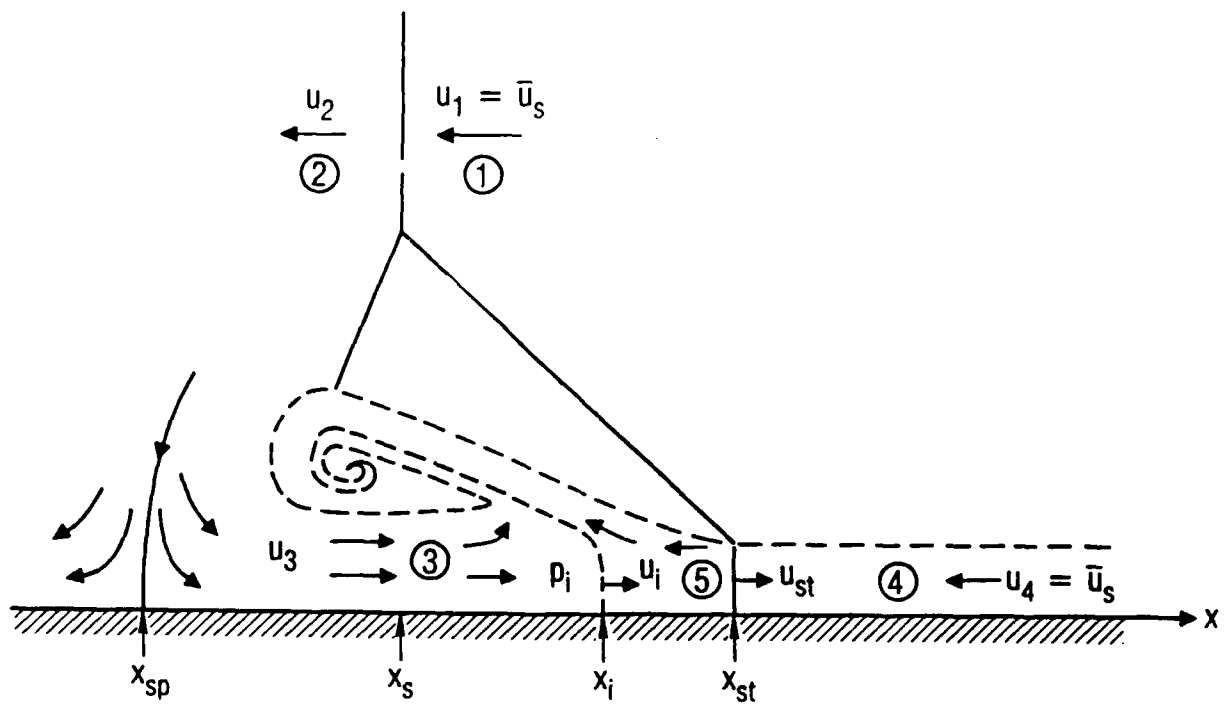


Fig. 2. Flow Conditions in Incident Shock Stationary Coordinate System at Early Times. Viscous effects are negligible, and the scale of the interaction grows linearly with time.<sup>8</sup>

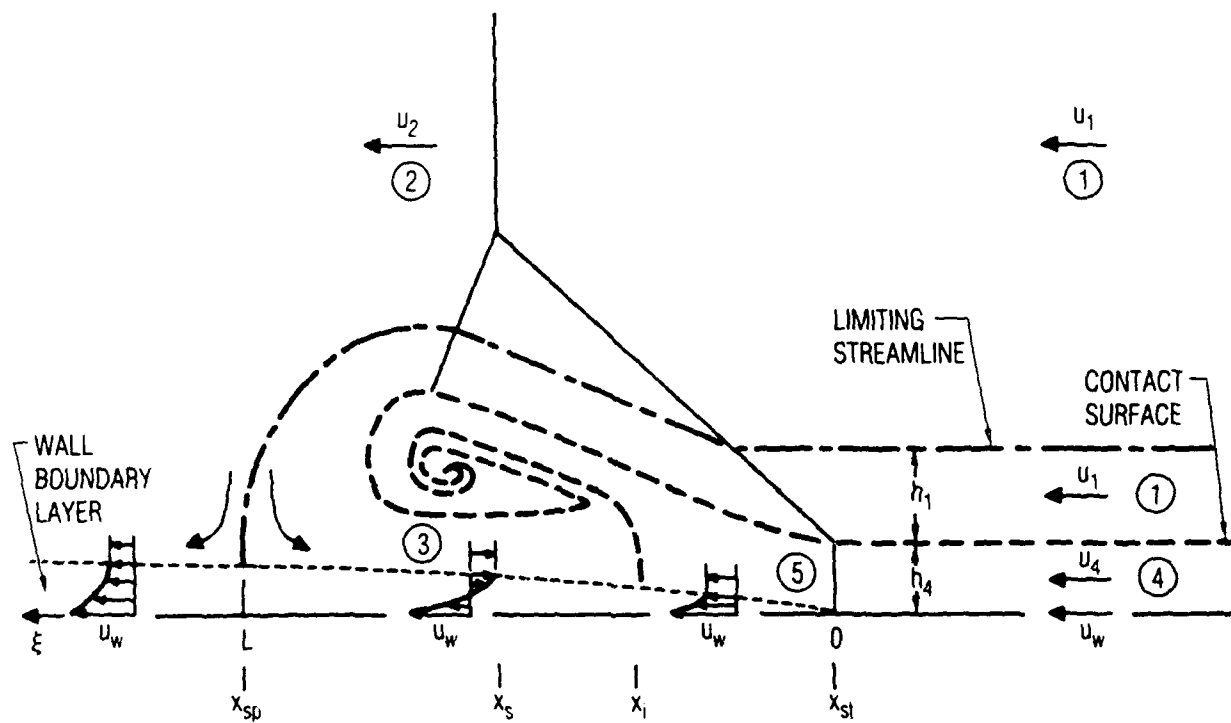


Fig. 3. Flow Conditions in Incident Shock Stationary Coordinate System at Late Times. Wall boundary layer flow is illustrated. The scale of the interaction is fixed, and the flow is steady.

the interaction region. The limiting streamline in Fig. 3 separates the free stream mass flow, which enters the bubble region, from the free stream mass flow, which does not enter the bubble region.

The asymptotic length of the interaction region, denoted  $L$ , is estimated in the following sections by equating the mass flow into and out of the bubble region.

The rate at which mass enters the bubble region (per unit width) may be written

$$\begin{aligned}\dot{m}_{in} &= \rho_4 u_4 h_4 + \rho_1 u_1 h_1 \\ &\equiv \rho_4 u_4 h_4 B\end{aligned}\tag{1}$$

where, noting  $u_1 = u_4$ ,

$$B = 1 + [(\rho_1 h_1)/(\rho_4 h_4)]$$

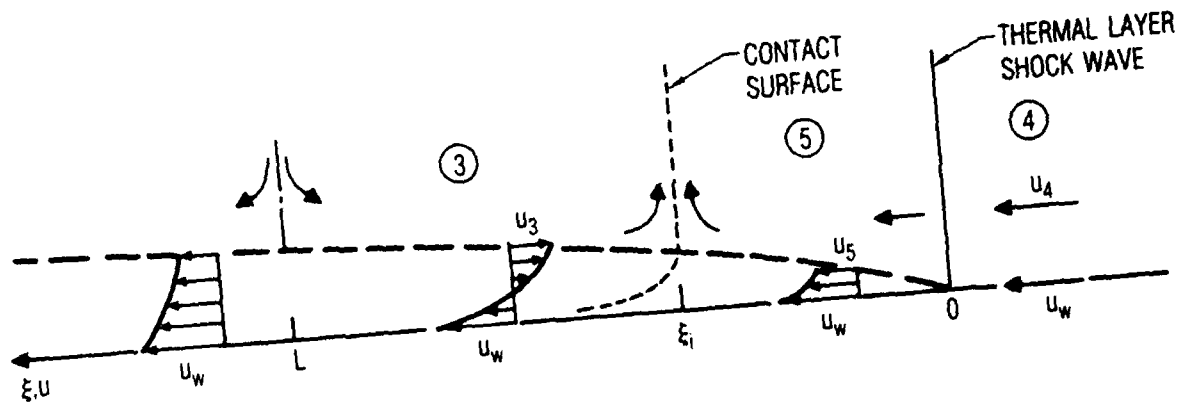
Here,  $h_4$  is the thickness of the thermal layer, and  $h_1$  is the thickness of the free stream layer that enters the bubble (Fig. 3). The quantity  $B$  is the ratio of total inflow to the inflow associated with the thermal layer. The quantity  $Bh_4$  may be viewed as an effective height of the thermal layer.

The wall boundary layer in Fig. 3 is reproduced in Fig. 4a. The solution of this boundary layer flow is complicated by the presence of the contact surface (which separates free stream particles from thermal layer particles) and by nonuniform boundary layer edge conditions. For present purposes, the boundary layer effect will be estimated by considering the limit  $u_e/u_w \rightarrow 0$  for a boundary layer with uniform edge conditions (Fig. 4b). This approach is accurate for the case of strong incident waves (wherein  $u_3/u_w$  and  $u_5/u_w$  are near zero) and provides an average edge condition for the case of weak incident waves. Distance from the shock wave in the thermal layer is denoted  $\xi$ .

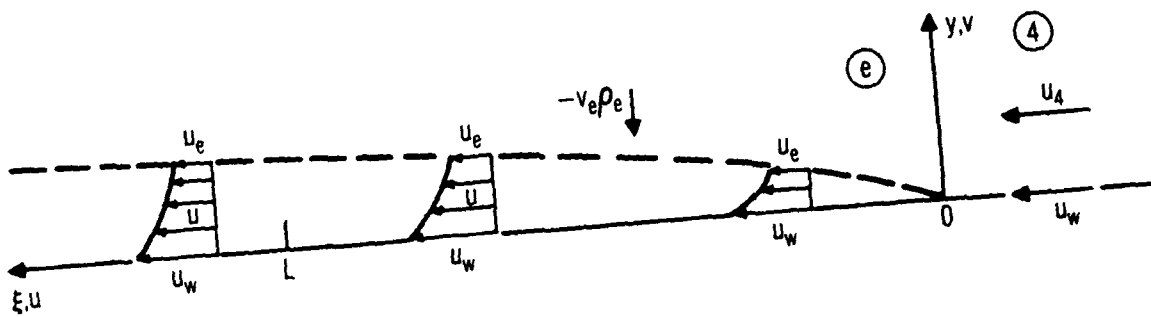
The excess mass flow in the boundary layer at any streamwise station is

$$\dot{m}_{bl} = \int_0^{\delta} (\rho u - \rho_e u_e) dy\tag{2}$$

where  $\delta$  is the local boundary layer thickness. The excess mass flow in the boundary layer may be expressed in the form



(a)



(b)

Fig. 4. Wall Boundary Layer in Incident Shock Fixed Coordinate System. (a) Schematic representation of actual flow external to boundary layer; (b) Assumption of uniform flow external to boundary layer.

$$\frac{\dot{m}_{bl}}{\rho_w u_w} = \frac{\rho_e u_e}{\rho_w u_w} (-\delta^*) \quad (3a)$$

where  $\delta^*$  is the boundary layer displacement thickness

$$\delta^* = \int_0^{\delta} \left(1 - \frac{\rho u}{\rho_e u_e}\right) dy \quad (3b)$$

The vertical velocity at the outer edge of the boundary layer is, from continuity considerations,

$$\rho_e v_e = - \frac{d\dot{m}_{bl}}{d\xi} = \rho_e u_e \left(-\frac{d\delta^*}{d\xi}\right) \quad (4)$$

Both  $\delta^*$  and  $v_e$  are negative for shock induced boundary layers.<sup>9</sup> Solutions for  $\delta^*$  and  $v_e$  are presented in Ref. 9 for the case of uniform flow external to the boundary layer. If it is assumed that the density and viscosity within the boundary layer are characterized by the wall values,  $\rho_w$  and  $\mu_w$ , the integral solution for  $\delta^*$  and  $v_e$  in Ref. 9 indicates that for  $\xi \leq \xi_t$

$$\frac{\dot{m}_{bl}}{\rho_w u_w \xi} = -2 \frac{\rho_e v_e}{\rho_w u_w} = 1.404 \left(\frac{v_w}{u_w \xi}\right)^{1/2} \quad (5a)$$

and, for  $\xi > \xi_t$

$$\frac{\dot{m}_{bl}}{\rho_w u_w (\xi - \xi_0)} = -\frac{5}{4} \frac{\rho_e v_e}{\rho_w u_w} = 0.1264 \left[\frac{v_w}{u_w (\xi - \xi_0)}\right]^{1/5} \quad (5b)$$

where Eqs. (5a) and (5b) apply for laminar and turbulent boundary layers, respectively. Here,  $\xi_0$  refers to the effective origin of the turbulent boundary layer, and  $\xi_t$  refers to the location of the transition from a laminar to a turbulent boundary layer (Fig. 5). The transition is assumed to be instantaneous and is assumed to occur at a known Reynolds number defined by

$$\frac{u_w \xi_t}{\nu_w} = Re_t \quad (6)$$

If it is assumed that  $\dot{m}_{bl}$  is continuous at  $\xi_t$ , the quantities  $\xi_0$  and  $\xi_t$  are related by

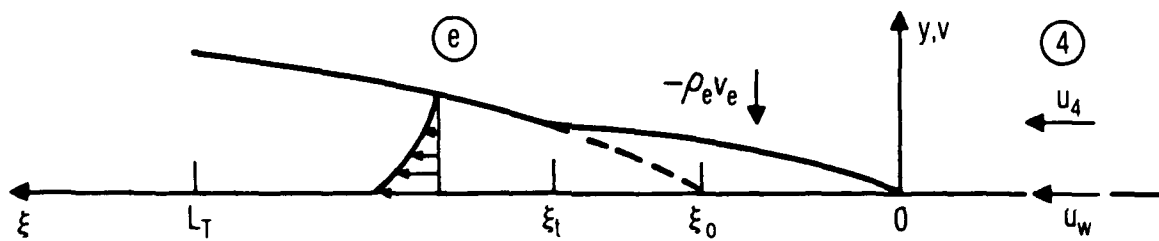


Fig. 5. Boundary Layer Development with Transition at  $\xi_t$  and with Effective Origin of Turbulent Boundary Layer at  $\xi_0$

$$\xi_0 = \xi_t (1 - 20.28 \text{Re}_t^{-3/8}) \quad (7)$$

Equations (5)-(7) define the excess mass flow in the boundary layer. Equating  $\dot{m}_{bl}$  and  $\dot{m}_{in}$  provides the length of the separation bubble. The result is, noting  $u_w = u_4 = u_1$ ,

$$\frac{v_1}{u_1 \text{Bh}_4} \frac{L_L}{\text{Bh}_4} = \left( \frac{\rho_4/\rho_w}{1.404} \right)^2 \frac{v_1}{v_w} \quad L_L \leq \xi_t \quad (8a)$$

$$\left( \frac{v_1}{u_1 \text{Bh}_4} \right)^{1/4} \frac{L_T - \xi_0}{\text{Bh}_4} = \left( \frac{\rho_4/\rho_w}{0.1264} \right)^{5/4} \left( \frac{v_1}{v_w} \right)^{1/4} \quad L_L > \xi_t \quad (8b)$$

where  $L_L$  and  $L_T$  denote the length of the laminar and the laminar plus turbulent bubble, respectively. The wall temperature  $T_w$  may be assumed to remain at its initial value  $T_4$ .<sup>9</sup> We also assume that regions 1 and 4 contain the same type of gas (e.g.,  $N_2/N_2$  rather than  $N_2/\text{He}$ ), and introduce the expressions

$$\frac{\rho_4}{\rho_w} = \frac{p_4}{p_w} \frac{T_w}{T_4} = \frac{p_1}{p_e} \quad (9a)$$

$$\mu \sim T^\omega \quad (9b)$$

$$\bar{M}_s = u_1/a_1 \quad (9c)$$

$$H \equiv 10^{-5} \times \text{Bh}_4 a_1/v_1 \quad (9d)$$

into Eq. (8). For laminar flow,  $L_L \leq \xi_t$ ,

$$\frac{1}{H} \frac{L_L}{\text{Bh}_4} = \frac{0.5073 \times 10^5}{p_e/p_1} \bar{M}_s (T_1/T_4)^{1+\omega} \quad (10a)$$

$$\frac{1}{H^2} \frac{L_L}{\xi_t} = \frac{0.5073 \times 10^{10}}{\text{Re}_t} \frac{\bar{M}_s^2}{(T_4/T_1)^{2(1+\omega)}} \quad (10b)$$

For turbulent flow,  $L_L > \xi_t$ ,

$$\frac{1}{H^{1/4}} \frac{L_T - \xi_0}{Bh_4} = \frac{236.0}{p_e/p_1} (\bar{M}_s)^{1/4} \left(\frac{T_1}{T_4}\right)^{(1+\omega)/4} \quad (11a)$$

$$H \frac{\xi_0}{Bh_4} = \frac{10^{-5} \times Re_t (T_4/T_1)^{1+\omega}}{(p_e/p_1) \bar{M}_s} \left(1 - \frac{20.28}{Re_t^{3/8}}\right) \quad (11b)$$

Finally, we assume that the bubble pressure  $p_e$  is equal to the stagnation pressure in region 5 of Fig. 3. For an ideal gas,

$$\frac{p_e}{p_1} = \frac{p_{5,t}}{p_4} = \left(1 + \frac{\gamma_4 - 1}{2} M_4^2\right)^{\gamma_4/(\gamma_4-1)} \quad M_4 \leq 1 \quad (12a)$$

$$= \left[\frac{(\gamma_4 + 1)M_4^2}{2}\right]^{\gamma_4/(\gamma_4-1)} \left(\frac{\gamma_4 + 1}{2\gamma_4 M_4^2 - \gamma_4 + 1}\right)^{1/(\gamma_4-1)} \quad M_4 > 1 \quad (12b)$$

Equations (10)-(12) can be evaluated by specification of  $\bar{M}_s$ ,  $T_4/T_1$ ,  $H$ ,  $Re_t$ ,  $\gamma_4$ , and  $\omega$ . Typically,

$$Re_t = 10^6 \quad (13)$$

and for air

$$\gamma_4 = 7/5 \quad (14a)$$

$$\omega = 0.7 \quad (14b)$$

$$\frac{a_1}{v_1} = 2.274 \times 10^5 p_1 \left(\frac{290}{T_1}\right)^{1.2} \text{ cm}^{-1} \quad (14c)$$

where  $p_1$  and  $T_1$  are in atmospheres and K, respectively. The quantity  $H$  is in the form of a Reynolds number and is of order 1 when  $Bh_4$  is of the order of a centimeter.

Numerical results are given in Table 1 and Fig. 6 for  $1.5 \leq \bar{M}_S \leq 6.0$ ,  $1.0 < a_4/a_1 \leq 3.4$ , and  $0.1 \leq H \leq 10$ . For each  $\bar{M}_S$ , the smallest value of  $a_4/a_1$  in Table 1 corresponds to the onset of the separation bubble. When  $H \ll 1$ , the boundary layer is wholly laminar and  $H^{-1} L_L/(Bh_4)$  is of order  $10^3$  to  $10^4$ . When  $H = 0.1$ , the boundary layer is laminar for the larger values of  $a_4/a_1$  and is laminar/turbulent for the smaller values of  $a_4/a_1$ . In the latter case,  $H^{-1/4} L_T/(Bh_4)$  is of order  $10^1$  to  $10^3$ , with the smaller values of  $H^{-1/4} L_T/(Bh_4)$  occurring at the larger value of  $\bar{M}_S$ . When  $Bh_4$  is of the order of 1 cm,  $H$  is of order 1 and the boundary layer is laminar/turbulent. The parameter  $H^{-1/4} L_T/(Bh_4)$  may be interpreted as defining the precursor length  $L_T$  in centimeters. The latter case then has values in the range  $8.5 \leq L_T, \text{ cm} \leq 412$  for  $\bar{M}_S \leq 6.0$  in Table 2. With increase of  $H$  beyond 10, the boundary layer is predominately turbulent and the parameter  $H^{-1/4} L_T/(Bh_4)$  becomes independent of  $H$ .

Table 1. Asymptotic Length of Thermal Precursor for Case  $Y_4 = 7/5$ ,  $\omega = 0.7$  and  $Re_T = 10^6$ .  
Laminar length  $L_L$  applies when 0.000 indicated for  $L_T$ .

$\bar{M}_s$	$\frac{a_4}{a_1}$	$\frac{P_2}{P_1}$	$M_4$	$\frac{P_e}{P_1}$	$\frac{1}{H^2} \frac{L_L}{\xi_t}$	$\frac{10^{-4} L_L}{H Bh_4}$	$\frac{10^{-2} L_T}{H^{1/4} Bh_4}$			
							H=0.1	H=1.0	H=10.0	
1.5	1.232	2.458	1.218	2.459	0.270E+04	1.522	1.758	0.939	0.892	0.890
	1.400	2.458	1.071	2.061	0.116E+04	1.176	2.563	1.042	0.957	0.953
	1.800	2.458	0.833	1.576	0.210E+03	0.654	5.921	1.282	1.021	1.000
	2.200	2.458	0.682	1.305	0.530E+02	0.382	0.000	1.611	1.015	0.981
	2.600	2.458	0.577	1.253	0.172E+02	0.236	0.000	2.140	0.994	0.929
	3.000	2.458	0.500	1.186	0.660E+01	0.153	0.000	2.952	0.983	0.872
3.400	2.458	0.441	1.143	0.279E+01	0.104	0.000	4.121	0.994	0.818	
2.0	1.135	4.500	1.762	4.498	0.859E+04	1.467	0.830	0.576	0.561	0.560
	1.200	4.500	1.667	4.081	0.587E+04	1.337	0.948	0.609	0.590	0.589
	1.400	4.500	1.429	3.150	0.206E+04	1.026	1.454	0.714	0.672	0.670
	1.800	4.500	1.111	2.162	0.375E+03	0.636	3.476	0.939	0.796	0.788
	2.200	4.500	0.909	1.708	0.952E+02	0.407	0.000	1.219	0.862	0.842
	2.600	4.500	0.769	1.479	0.306E+02	0.266	0.000	1.614	0.886	0.845
3.000	4.500	0.667	1.347	0.116E+02	0.180	0.000	2.197	0.896	0.823	
3.400	4.500	0.588	1.264	0.493E+01	0.125	0.000	3.032	0.911	0.792	
2.5	1.101	7.125	2.271	7.122	0.165E+05	1.284	0.507	0.391	0.384	0.384
	1.200	7.125	2.083	6.076	0.918E+04	1.123	0.611	0.429	0.419	0.418
	1.400	7.125	1.786	4.604	0.322E+04	0.877	0.914	0.508	0.486	0.484
	1.800	7.125	1.389	3.011	0.582E+03	0.571	2.143	0.686	0.603	0.598
	2.200	7.125	1.136	2.229	0.149E+03	0.390	4.808	0.913	0.694	0.682
	2.600	7.125	0.962	1.811	0.478E+02	0.272	0.000	1.232	0.766	0.729
3.000	7.125	0.833	1.576	0.181E+02	0.192	0.000	1.682	0.793	0.743	
3.400	7.125	0.736	1.432	0.771E+01	0.138	0.000	2.319	0.821	0.737	
3.0	1.084	10.333	2.768	10.337	0.264E+05	1.119	0.347	0.284	0.281	0.281
	1.200	10.333	2.500	8.526	0.132E+05	0.960	0.427	0.318	0.312	0.312
	1.400	10.333	2.143	6.398	0.463E+04	0.768	0.622	0.379	0.366	0.365
	1.800	10.333	1.667	4.081	0.839E+03	0.505	1.411	0.515	0.465	0.462
	2.200	10.333	1.364	2.924	0.214E+03	0.357	3.165	0.691	0.552	0.544
	2.600	10.333	1.154	2.277	0.608E+02	0.260	0.000	0.940	0.624	0.607
3.000	10.333	1.000	1.893	0.260E+02	0.192	0.000	1.299	0.682	0.647	
3.400	10.333	0.892	1.659	0.111E+02	0.143	0.000	1.903	0.726	0.665	
3.5	1.075	14.125	3.256	14.119	0.380E+05	0.983	0.256	0.217	0.215	0.215
	1.200	14.125	2.917	11.427	0.180E+05	0.836	0.315	0.246	0.242	0.242
	1.400	14.125	2.500	8.526	0.631E+04	0.663	0.450	0.294	0.285	0.285
	1.800	14.125	1.944	5.360	0.114E+04	0.449	0.985	0.367	0.366	0.366
	2.200	14.125	1.591	3.768	0.292E+03	0.323	2.182	0.536	0.444	0.439
	2.600	14.125	1.346	2.866	0.937E+02	0.241	0.000	0.728	0.513	0.501
3.000	14.125	1.167	2.312	0.354E+02	0.183	0.000	1.007	0.575	0.550	
3.400	14.125	1.029	1.900	0.151E+02	0.141	0.000	1.411	0.629	0.585	

Table 1. Asymptotic Length of Thermal Precursor for Case  $\gamma_4 = 7/5$ ,  $\omega = 0.7$  and  $Re_t = 10^6$ .  
Laminar length  $L_L$  applies when 0.000 indicated for  $L_T$ . (Cont'd)

$\bar{M}_s$	$\frac{a_4}{a_1}$	$\frac{P_2}{P_1}$	$M_4$	$\frac{P_e}{P_1}$	$\frac{1}{H^2} \frac{L_L}{\xi_L}$	$\frac{10^{-4} L_L}{H Bh_4}$	$\frac{10^{-2} L_T}{H^{1/4} Bh_4}$			
							H=0.1	H=1.0	H=10.0	H=100.0
4.0	1.009	18.500	3.742	18.498	0.510E+05	0.874	0.197	0.172	0.171	0.171
	1.200	18.500	3.333	14.777	0.235E+05	0.739	0.243	0.196	0.194	0.193
	1.400	18.500	2.857	10.985	0.824E+04	0.588	0.341	0.235	0.229	0.228
	1.800	18.500	2.222	6.842	0.149E+04	0.402	0.721	0.320	0.297	0.296
	2.200	18.500	1.818	4.753	0.381E+03	0.292	1.569	0.427	0.363	0.359
	2.600	18.500	1.538	3.561	0.122E+03	0.221	3.265	0.576	0.425	0.417
5.0	3.000	18.500	1.333	2.822	0.462E+02	0.172	0.000	0.794	0.483	0.466
	3.400	18.500	1.176	2.340	0.197E+02	0.135	0.000	1.111	0.538	0.506
	1.062	29.000	4.708	29.005	0.842E+05	0.713	0.129	0.116	0.116	0.116
	1.200	29.000	4.167	22.820	0.367E+05	0.598	0.158	0.134	0.133	0.132
	1.400	29.000	3.571	16.892	0.129E+05	0.478	0.216	0.160	0.157	0.157
	1.800	29.000	2.778	10.410	0.233E+04	0.330	0.429	0.218	0.206	0.206
6.0	2.200	29.000	2.273	7.134	0.595E+03	0.244	0.898	0.289	0.255	0.253
	2.600	29.000	1.923	5.255	0.191E+03	0.187	1.843	0.385	0.303	0.298
	3.000	29.000	1.667	4.081	0.722E+02	0.148	0.000	0.522	0.350	0.341
	3.400	29.000	1.471	3.303	0.308E+02	0.120	0.000	0.722	0.397	0.379
	1.059	41.833	5.666	41.795	0.124E+06	0.599	0.092	0.085	0.084	0.084
	1.200	41.833	5.000	32.653	0.529E+05	0.501	0.112	0.098	0.097	0.097
1.400	41.833	4.286	24.115	0.185E+05	0.402	0.149	0.117	0.115	0.115	
1.800	41.833	3.333	14.777	0.336E+04	0.279	0.283	0.159	0.152	0.152	
2.200	41.833	2.727	10.053	0.857E+03	0.207	0.569	0.209	0.189	0.188	
2.600	41.833	2.308	7.339	0.275E+03	0.161	1.145	0.275	0.226	0.224	
3.000	41.833	2.000	5.640	0.104E+03	0.129	2.208	0.367	0.264	0.258	
3.400	41.833	1.765	4.509	0.444E+02	0.105	0.000	0.500	0.301	0.290	

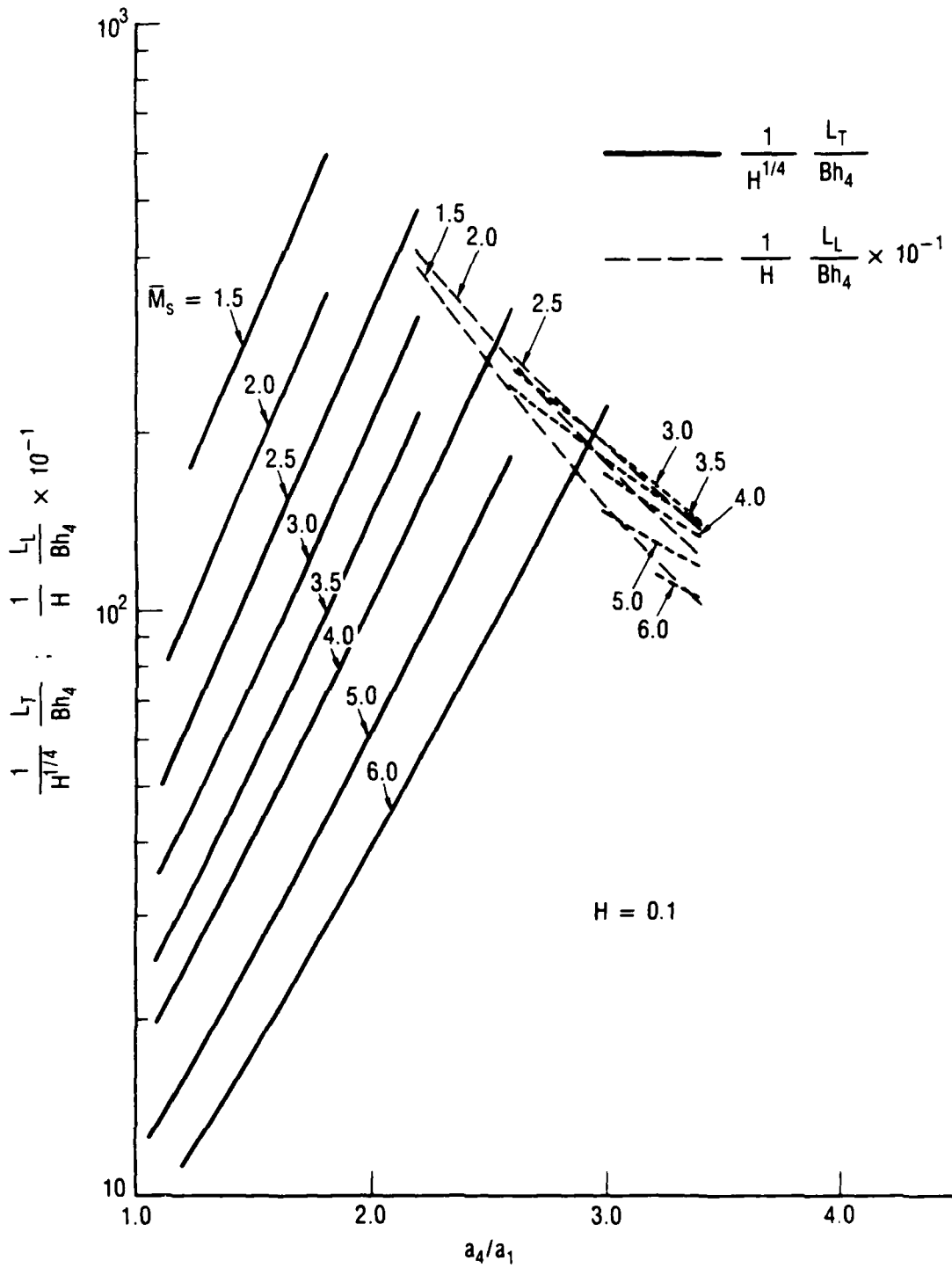


Fig. 6. Streamwise Length of Separation Bubble for Case  $\gamma_4 = 7/5$ ,  $\omega = 0.7$ , and  $Re_t = 10^6$ . (a)  $H = 0.1$ .

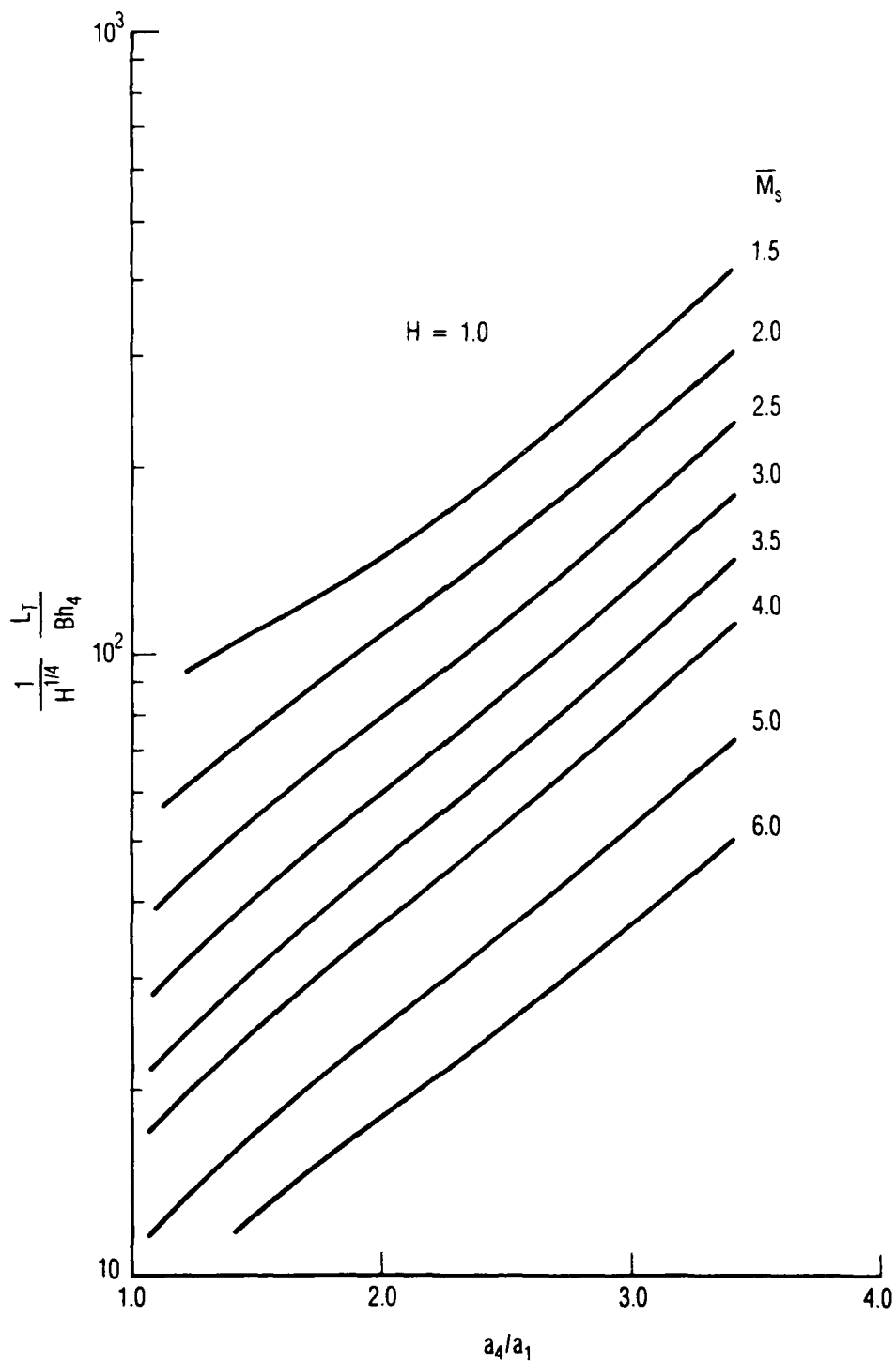


Fig. 6. Streamwise Length of Separation Bubble for Case  $\gamma_4 = 7/5$ ,  $\omega = 0.7$ , and  $Re_t = 10^6$ . (b)  $H = 1.0$ .

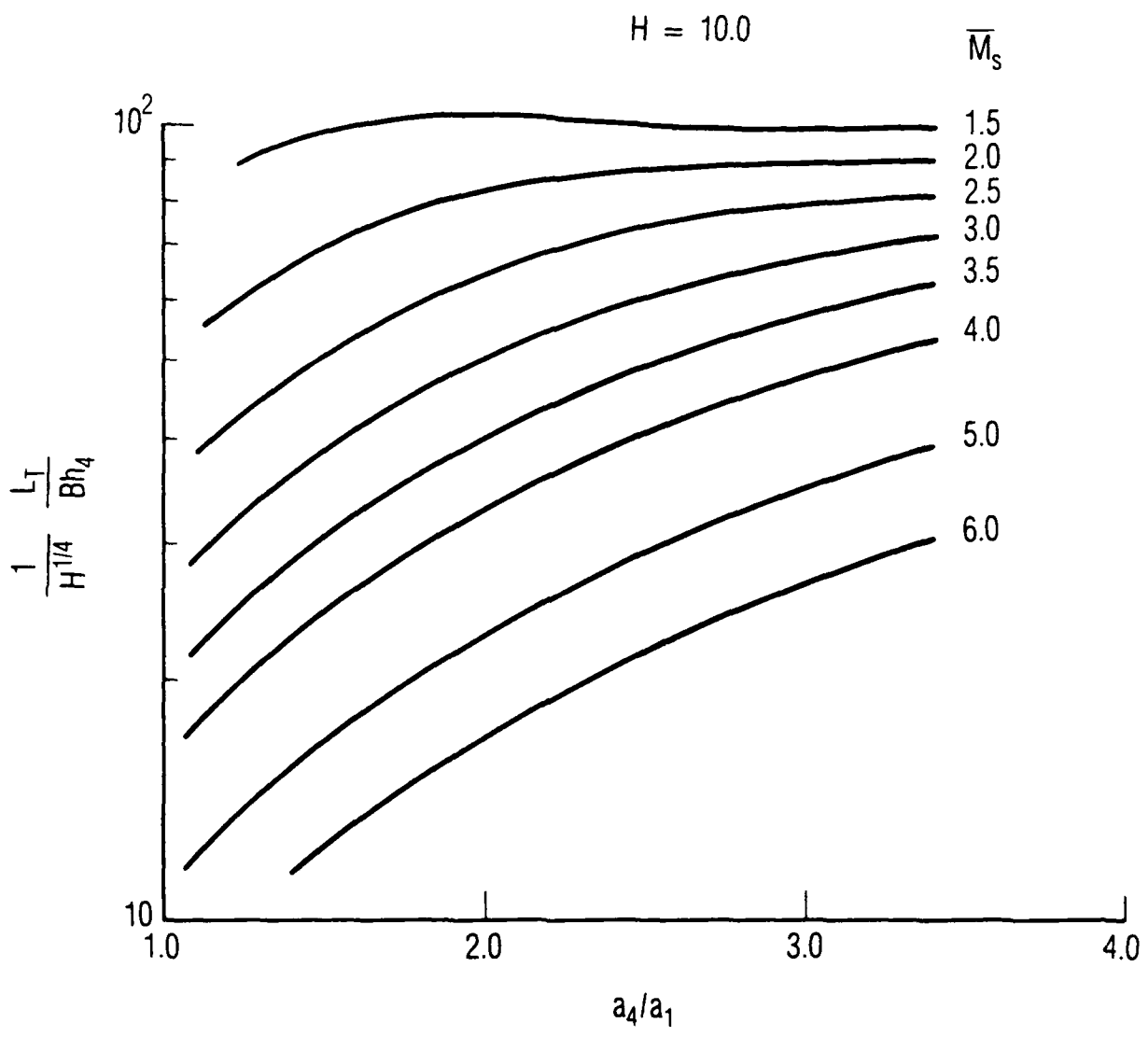


Fig. 6. Streamwise Length of Separation Bubble for Case  $\gamma_4 = 7/5$ ,  $\omega = 0.7$ , and  $Re_t = 10^6$ . (c)  $H = 10.0$ .

Table 2. Characteristic Time to Reach Steady State  
for Case  $\gamma_1 = \gamma_4 = 7/5$

$\bar{M}_s$	$\frac{a_4}{a_1}$	$\frac{\bar{u}_i}{a_4}$ Ref. 8	$\frac{\bar{u}_s t_c}{L_{L,T}}$ Eq. 18
1.500	1.232	1.461	5.001
1.500	1.400	1.405	3.212
1.500	1.800	1.252	1.990
1.500	2.200	1.110	1.592
1.500	2.600	0.989	1.400
1.500	3.000	0.886	1.295
1.500	3.400	0.800	1.230
2.000	1.135	1.975	8.277
2.000	1.200	1.950	5.882
2.000	1.400	1.851	3.382
2.000	1.800	1.632	2.133
2.000	2.200	1.438	1.719
2.000	2.600	1.278	1.512
2.000	3.000	1.147	1.388
2.000	3.400	1.037	1.311
2.500	1.101	2.478	10.952
2.500	1.200	2.429	6.027
2.500	1.400	2.294	3.513
2.500	1.800	2.006	2.251
2.500	2.200	1.760	1.822
2.500	2.600	1.560	1.607
2.500	3.000	1.398	1.476
2.500	3.400	1.264	1.391

### III. TIME TO REACH STEADY STATE

We now estimate the time to reach steady state for the interaction of a shock with a thin semi-infinite thermal layer (Fig. 1). The bubble growth rate is most rapid at small times, when the interaction is essentially inviscid. It is this small time growth rate that is used to characterize the overall rate of bubble growth.

The inviscid solution of Ref. 8 provides numerical estimates for the unsteady streamwise separation between the interface and the incident shock, namely,

$$x_i - x_s = t (\bar{u}_i - \bar{u}_s) \quad (15)$$

where  $\bar{u}_i/a_4$  is tabulated as a function of  $\bar{M}_s$  and  $a_4/a_1$  in Ref. 8. The time for this separation distance to reach a value  $L_{L,T}$  is denoted  $t_c$  and is given by

$$\frac{\bar{u}_s t_c}{L_{L,T}} = \left( \frac{1}{\bar{M}_s} \frac{a_4}{a_1} \frac{\bar{u}_i}{a_4} - 1 \right)^{-1} \quad (16)$$

when  $L_{L,T}$  denotes either  $L_L$  or  $L_T$ . The time  $t_c$  is assumed herein to characterize the time required to reach the asymptotic steady state flow. Note that the product  $\bar{u}_s t_c$  characterizes the distance the shock moves during the unsteady portion of the interaction.

Numerical results for  $\bar{u}_s t_c / L_{L,T}$  are given in Table 2. This parameter is of order 10 for values of  $a_4/a_1$  that correspond to the onset of separation, and approaches a value of order 1 with increase in  $a_4/a_1$ .

#### IV. APPLICATION TO NUMERICAL CODES

The present theory suggests a method by which wall viscous effects can be incorporated into inviscid codes. For the case of a flow that is steady in shock fixed coordinates, the inviscid code wall boundary condition  $v_e = 0$  can be replaced by the condition, from Eqs. (5a) and (5b),

$$\frac{\rho_e v_e}{\rho_1 \bar{u}_s} = - A_L \left( \frac{h_4}{\xi} \right)^{1/2} \quad \xi \leq \xi_t \quad (17a)$$

$$= - A_T \left( \frac{h_4}{\xi - \xi_0} \right)^{1/5} \quad \xi > \xi_t \quad (17b)$$

where

$$\xi_t = Re_t v_w / \bar{u}_s \quad (17c)$$

$$\xi_0 = \xi_t (1 - 20.28 Re_t^{-3/8}) \quad (17d)$$

and, for the same gas in regions 1 and 4,

$$\frac{v_w}{\bar{u}_s} = \left[ \left( \frac{T_4}{T_1} \right)^{\omega+1} \frac{v_1}{\bar{M}_s a_1} \right] \frac{p_1}{p_e} \quad (17e)$$

$$A_L = 0.702 \left[ \frac{p_e}{p_1} \left( \frac{T_1}{T_4} \right)^{1-\omega} \frac{v_1}{a_1 h_4 \bar{M}_s} \right]^{1/2} \quad (17f)$$

$$A_T = 0.1011 \left[ \left( \frac{p_e}{p_1} \right)^4 \left( \frac{T_1}{T_4} \right)^{4-\omega} \frac{v_1}{a_1 h_4 \bar{M}_s} \right]^{1/5} \quad (17g)$$

The quantity  $p_e/p_1$  is evaluated from Eq. (12a). For  $M_4 > 1$ , the origin of the  $\xi$  coordinate system is taken to be at the shock in the thermal layer. For  $M_4 \leq 1$ , the origin is taken at the streamwise location where a prescribed pressure increment has occurred.

Numerical code calculations (either viscous codes or inviscid codes with prescribed  $\rho_e v_e \neq 0$ ) provide a basis for estimating the parameter B, which was introduced in Eq. (1). Thus, if  $L_L$  and  $L_T$  denote steady-state bubble length values obtained from numerical codes, the corresponding values of B are

$$B = 2 A_L \frac{T_4}{T_1} \left( \frac{L_L}{h_4} \right)^{1/2} \quad L_L \leq \xi_t \quad (18a)$$

$$= \frac{5}{4} A_T \frac{T_4}{T_1} \left( \frac{L_T - \xi_0}{h_4} \right)^{4/5} \quad L_T > \xi_t \quad (18b)$$

Hopefully, B is a weak function of initial conditions. The numerical code calculations can also be used to obtain improved estimates for  $t_c$ .

## V. CONCLUDING REMARKS

The present study represents a first attempt to analytically estimate the asymptotic streamwise length of the separation bubble associated with the interaction between a moving shock and a thin stationary thermal layer. Parameters and qualitative trends are identified. As previously noted, further study incorporating numerical code computation is needed to provide more accurate estimates of the asymptotic bubble length and of the time to reach steady state flow. It has been assumed in Eqs. (9a)-(9d) that regions 1 and 4 contain the same gas but at different temperatures. The role of dissimilar gases (e.g.,  $N_2/He$ ) also requires further study.

The present study indicates the importance of viscous effects on precursor development and provides a method for modifying the wall boundary condition in inviscid numerical codes in order to include the effect of the wall boundary layer on the inviscid flow. Equations (17a)-(17g) are approximately correct for cases where the flow is steady in incident shock fixed coordinates. The expressions for  $\rho_e v_e$  in Eqs. (17a) and (17b) require modification for cases where the flow is unsteady in shock fixed coordinates.

#### REFERENCES

1. R. V. Hess, Interaction of Moving Shocks and Hot Layers, TN 4002, NACA, Washington, D.C. (1957).
2. W. C. Griffith, "Interaction of a Shock Wave with a Thermal Boundary Layer," J. Aero. Sci., 16-22 (January 1956).
3. E. J. Gion, "Plane Shock Interacting with Thermal Layer," Phys. Fluids 20 (4), 700-702 (April 1977).
4. H. Reichenback and A. L. Kuhl, "Simulation of Precursors in Shock Tubes," Proceedings of the 16th Int. Symp. on Shock Tubes and Waves (Aachen, West Germany, 26-31 July 1987), ed. H. Gronig, VCH, Weinheim, Germany (1988), pp. 847-853.
5. G. P. Schneyer and D. E. Wilkins, Thermal Layer-Shock Interaction (Precursor) Simulation Data Book, Report No. SSS-R-84-6584, S-Cubed, La Jolla CA (March 1984).
6. W. S. Glowaki, A. L. Kuhl, H. M. Glaz, and R. E. Ferguson, "Shock Wave Interaction with High Sound Speed Layers," Proceedings of the 15th Int. Symposium on Shock Waves and Shock Tubes (Berkeley, CA, 18 July-2 August 1985), eds. D. Bershader and R. Hanson, Stanford University Press, Stanford, CA (1986).
7. M. A. Fry and D. L. Book, "Shock Dynamics in Heated Layers," Proceedings of the 15th Int. Symposium on Shock Wave and Shock Tubes (Berkeley, CA, 28 July-2 August 1985), eds. D. Bershader and R. Hanson, Stanford University Press, Stanford CA (1986).
8. H. Mirels, "Interaction of Moving Shock with Thin Stationary Layer," Proceedings of the 16th Int. Symposium on Shock Tubes and Waves (Aachen, West Germany, 26-31 July 1987), ed. H. Gronig, VCH, Weinheim, Germany (1988).
9. H. Mirels, Boundary Layer Behind Shock or Thin Expansion Wave Moving into Stationary Fluid, TN 1712, NACA, Washington, D.C. (May 1956).

## APPENDIX

### SYMBOLS

a	speed of sound
B	ratio of total flow to thermal layer flow into separation bubble, Eq. (1)
H	normalized thermal layer height, $10^{-5} B h_4 a_1 / \nu_1$
$h_1$	thickness of free stream layer that enters separation bubble, Fig. 3
$h_4$	height of thermal layer, Fig. 3
$L_L, L_T$	length of separation bubble for laminar and laminar/turbulent boundary layers, respectively
$\bar{M}_S$	shock Mach number in wall stationary coordinate system, $\bar{u}_s / a_1$
$M_4$	Mach number of flow in thermal layer in incident shock stationary coordinates, $u_4 / a_4 = (a_1 / a_4) \bar{M}_S$
$\dot{m}_{in}$	mass rate of flow into separation bubble, Eq. (1)
$\dot{m}_{bl}$	excess mass flow rate in wall boundary layer, Eq. (2)
p	static pressure
t	time
$t_c$	characteristic time to establish steady flow, Eq. (16)
$\bar{u}$	streamwise velocity in wall stationary coordinate system, Fig. 1
u	streamwise velocity in incident shock stationary coordinate system, Fig. 2.
$u_w$	wall velocity in incident shock stationary coordinate systems, Fig. 3
$v_e$	velocity in +y direction at edge of boundary layer
x	streamwise distance measured from leading edge of thermal layer, Fig. 1
$x_{st}, x_i, x_s, x_{sp}$	location of shock in thermal layer, interface, incident shock, and stagnation point, respectively, Fig. 2.
y	distance normal to wall
$\gamma$	ratio of specific heats $c_p / c_v$
$\delta$	boundary layer thickness
$\delta^*$	boundary layer displacement thickness, Eq. (3b)
$\mu$	viscosity
$\nu$	kinematic viscosity, $\mu / \rho$
$\xi$	distance measured from shock in thermal layer, $x_{st} - x$

APPENDIX (continued)

$\rho$  density  
 $w$  viscosity exponent,  $\mu \sim T^w$

Subscripts

1,2,  
3,4, flow regions, Fig. 2  
5

e edge of boundary layer  
w property at wall

Superscripts

$\bar{M}, \bar{u}$  barred quantities are in wall fixed coordinate system  
 $M, u$  unbarred quantities are in incident shock fixed coordinate system